Available online at www.sciencedirect.com
ScienceDirect
Phytochemistry 69 (2008) 240–251
PHYTOCHEMISTRY
www.elsevier.com/locate/phytochem

LC–MS and GC–MS metabolite profiling of nickel(II) complexes in the latex of the nickel-hyperaccumulating tree *Sebertia acuminata* and identification of methylated aldaric acid as a new nickel(II) ligand

Damien L. Callahan [a], Ute Roessner [b], Vincent Dumontet [c], Nicolas Perrier [d,1], Anthony G. Wedd [a,e], Richard A.J. O'Hair [a,e], Alan J.M. Baker [f], Spas D. Kolev [a,*]

[a] *School of Chemistry, The University of Melbourne, Victoria 3010, Australia*
[b] *Australian Centre for Plant Functional Genomics, School of Botany, The University of Melbourne, Victoria 3010, Australia*
[c] *Institut de Chimie des Substances Naturelles, Centre National de la Recherche Scientifique, 91198 Gif-sur-Yvette Cedex, France*
[d] *Institut de Recherche pour le Développement, 98848 Nouméa, New Caledonia*
[e] *Bio21 Molecular Science and Biotechnology Institute, The University of Melbourne, Victoria 3010, Australia*
[f] *School of Botany, The University of Melbourne, Victoria 3010, Australia*

Received 2 April 2007; received in revised form 4 July 2007
Available online 4 September 2007

Abstract

Targeted liquid chromatography–mass spectrometry (LC–MS) technology using size exclusion chromatography and metabolite profiling based on gas chromatography–mass spectrometry (GC–MS) were used to study the nickel-rich latex of the hyperaccumulating tree *Sebertia acuminata*. More than 120 compounds were detected, 57 of these were subsequently identified. A methylated aldaric acid (2,4,5-trihydroxy-3-methoxy-1,6-hexan-dioic acid) was identified for the first time in biological extracts and its structure was confirmed by 1D and 2D nuclear magnetic resonance (NMR) spectroscopy. After citric acid, it appears to be one of the most abundant small organic molecules present in the latex studied. Nickel(II) complexes of stoichiometry Ni^{II}:acid = 1:2 were detected for these two acids as well as for malic, itaconic, erythronic, galacturonic, tartaric, aconitic and saccharic acids. These results provide further evidence that organic acids may play an important role in the transport and possibly in the storage of metal ions in hyperaccumulating plants.

Keywords: *Sebertia acuminata*; Hyperaccumulator; Organic acid; Ni^{II} complex; Metabolite profiling; LC–MS; GC–MS

1. Introduction

Nickel concentrations of up to 26% dry mass have been detected in the latex from the tree *Sebertia acuminata* Pierre ex Baill. (Sapotaceae) (Jaffré et al., 1976). This is the highest concentration of nickel found in any organism and a single tree may contain 37 kg of the metal (Sagner et al., 1998). *S. acuminata* is a rare rainforest tree endemic to New Caledonia and is generally found in Ni-rich ultramafic serpentine soils in southern parts of the island. It belongs to a diverse group of plants known as hyperaccumulators which store metal ions in their above-ground tissues at levels which are toxic to other species. As the Ni concentration in a normal plant is less than 0.001%, a plant which exceeds 0.1% Ni dry mass is classed as a Ni hyperaccumulator.

The physiology of nickel in plants has been reviewed recently (Seregin and Kozhevnikova, 2006). This element is essential in some species as it is a constituent of the hydrolytic enzyme urease (Dixon et al., 1975; Eskew et al., 1983). The physiological reasons for hyperaccumulation are not well understood. High concentrations of metals normally cause oxidative damage and inhibition of enzyme function and so excess metal ions are sequestered and stored. Hyperaccumulation may be an ecological

* Corresponding author. Tel.: +61 3 8344 793l; fax: +61 3 9347 5180.
E-mail address: s.kolev@unimelb.edu.au (S.D. Kolev).
[1] Deceased June 2006.

0031-9422/$ - see front matter © 2007 Elsevier Ltd. All rights reserved.
doi:10.1016/j.phytochem.2007.07.001

adaptation by growth on metalliferous soils. There is more nickel in the latex of *S. acuminata* than in the leaves and so Ni^{2+} ions may be deposited in the latex as a waste product as it has been suggested before that latex may function as a waste repository (Shukla and Krishna Murti, 1971). Other plants may have developed methods of exclusion to deal with the metalliferous soils (Baker, 1981).

Other taxa with Ni-rich latex include *Euphorbia helenae* Urb. subsp. *grandifolia* Borhidi and Muñiz from Cuba and *Cnidoscolus* (Jatropha) sp.nov found in Brazil. It has been proposed that hyperaccumulation could provide protection from attack by fungi or herbivores (Boyd, 1998; Davis et al., 2001; Hanson et al., 2004) and such protection has also been observed in plants which hyperaccumulate Ni (Boyd and Martens, 1994; Jhee et al., 2005). The high metal concentration in the latex of *S. acuminata* has a repellent effect on the fruit fly *Drosophila melanogaster* (Sagner et al., 1998).

The ligands which bind metal ions in hyperaccumulators have not been well characterised (Callahan et al., 2006). The fact that *S. acuminata* can amass such extreme metal concentrations in the latex implies the existence of a metal transport/detoxification mechanism involving selective ligands. A correlation between Ni and citric acid concentrations in leaves has been demonstrated in a range of hyperaccumulating species (Lee et al., 1978). Previous studies of the *S. acuminata* latex have reported that between 37% and 99% of the Ni is complexed by citric acid $C_6H_8O_7 = H_4cit$ (Sagner et al., 1998; Schaumlöffel et al., 2003). The complex cation $[Ni^{II}(H_3cit)(H_4cit)]^+$ was identified in the gas phase following electrospray ionisation of eluant from water extracts of the latex (Schaumlöffel et al., 2003). As citrate does not bind Ni^{2+} strongly ($\lg K = 5.4$, where K is the association constant of the complex), the Ni^{2+} ion may be transported to the laticifers in the form of its more stable complexes with nicotianamine ($\lg K = 16.1$) (Schaumlöffel et al., 2003) or histidine ($\lg K = 8.7$) (Martell and Smith, 1974).

The present paper reports on a detailed phytochemical study of the latex of *S. acuminata* involving metabolic profiling and the identification of a new Ni^{2+} binding ligand. As latex simply exudes from bark incisions, collection and processing is simplified making it an ideal material to study Ni^{2+} coordination in hyperaccumulators. This approach minimises the danger of identifying ligands which are not involved in metal binding *in vivo* as could be the case with chemical extraction of homogenised leaf material.

2. Results and discussion

2.1. General approach

Using GC–MS based metabolite profiling a list of compounds present within the latex of *S. acuminata* was produced as the chemical composition of this unique biological fluid was unknown. GC–MS was applied to separate low molar mass compounds. These were identified by comparing their mass spectral fragmentation patterns and retention indices with the National Institute of Standards and Technology (NIST) mass spectral library (version 2.0) and the public domain mass spectral library of the Max Planck Institute for Molecular Plant Physiology (Golm, Germany) (MSRI; NIST; Kopka et al., 2005). These data were used later to identify Ni^{II} complexes in the LC–MS spectra. The metabolite profile was also used to identify other possible ligands that either dissociated from their Ni^{II} complexes during the LC separation, or were not detected due to ion suppression under the electrospray ionisation (ESI) conditions used.

The main objective of this study was to extend the work by Schaumlöffel et al. (2003) by identifying ligands other than citrate bound to Ni^{2+} within the latex of *S. acuminata*. LC–MS was used to identify ionic Ni^{II} complexes in the gas phase via the unique isotope pattern of elemental nickel. One such ion, which could not be identified on the basis of the GC–MS measurements, was detected. The isolation of the corresponding ligand was required for its full characterisation. Isolation was carried out using semi-preparative HPLC. The isolated ligand was then characterised using MS, including collisional induced dissociation (CID) and high resolution MS, and by 1D and 2D NMR spectroscopy. The identity of other Ni^{II} complexes was confirmed by the MS analysis of synthetic solutions.

2.2. Ni concentrations in the S. acuminata latex and associated soil

Fig. 1 shows the bright green/blue latex exuding from an incision in the bark of an *S. acuminata* tree. The samples were collected from six trees in two locations in southern New Caledonia. The mean and standard deviation for the Ni concentration in the six latex samples was 63.5 ± 8.0 g/kg fresh mass. The ultramafic soil in the two locations where the latex samples were collected is formed mainly from goethite and hematite (Perrier et al., 2004). These soils possess amongst the highest concentrations of Ni in the world and hence this area of New Caledonia is under intense pressure from mining (L'Huillier and Edighoffer, 1996). The total soil Ni concentration determined in the *aqua regia* digests in the two locations for latex sampling was found to be 5.2 ± 0.3 g/kg dry mass and 6.3 ± 0.3 g/kg dry mass ($n = 3$, 95% confidence level). The 1,1,4,7,7-diethylene-triaminepentaacetic acid (DTPA)-extractable Ni, considered to be a good indication of Ni bioavailability in ultramafic soils (L'Huillier and Edighoffer, 1996), was 730 and 210 mg/kg. These results suggest that a substantial concentration factor of approximately two orders of magnitude is involved in the transfer of Ni from the soil to storage in the latex vessels.

2.3. GC–MS based metabolite profiling of the latex

Each of the six latex samples was studied by GC–MS. After AMDIS deconvolution (AMDIS) the chromato-

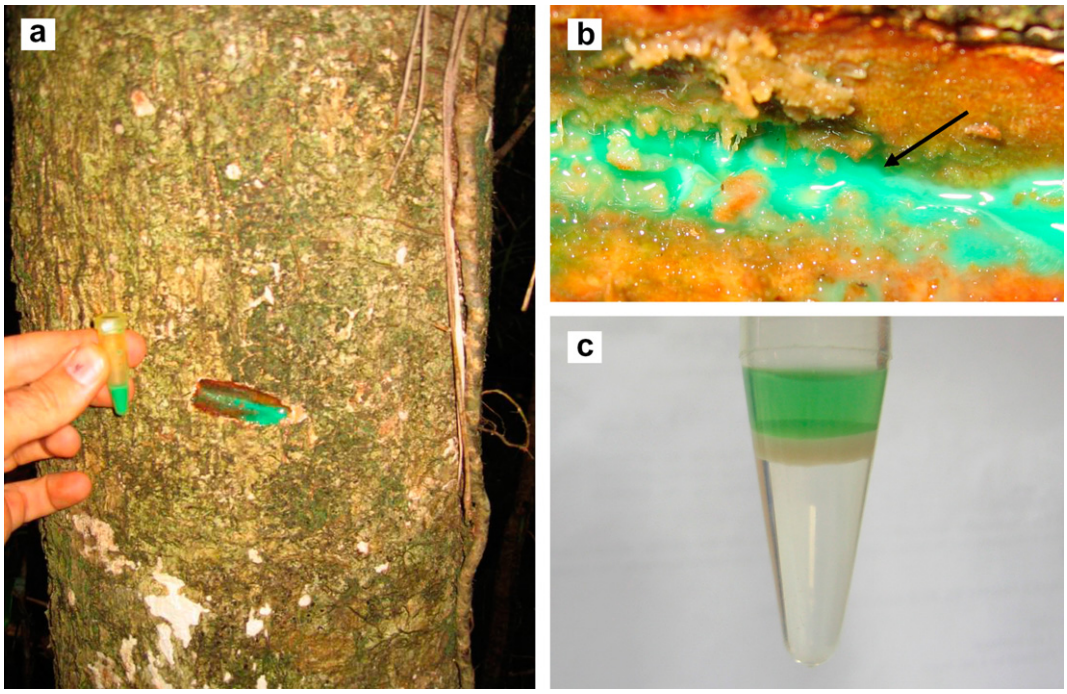

Fig. 1. (a) Collection of Ni-rich latex from *S. acuminata*; (b) close-up image of the exuded latex after incision. Note the separation of the green aqueous phase from the latex emulsion (see arrow); (c) the bright green aqueous extract resulting from a simple aqueous/chloroform separation of the latex.

grams and the accompanying mass spectra suggested the presence of at least 120 individual compounds. The NIST and Golm mass spectral libraries (Kopka et al., 2005) were searched for matching retention indices and mass spectra and 65 separate compounds were identified. The area of each chromatographic peak for the metabolites in each sample was determined and the relative response ratios (RRR) per gram fresh mass were calculated. The RRR was calculated as the metabolite area divided by both the internal standard area and the sample mass (Roessner et al., 2006). Table 1 lists the RRR of the metabolites identified in the six samples. The considerable variation in the RRR for some of the compounds studied between the six samples could be possibly attributed to natural variation between the samples.

In addition to citric acid, known to be the most abundant metabolite (Sagner et al., 1998; Schaumlöffel et al., 2003) the following organic acids were also identified: malic, aconitic, erythronic, galacturonic, tartaric, quinic, gluconic and saccharic acid. Each of these acids can coordinate Ni^{2+} weakly ($\lg K$, 1.8–4.2; Table 1). An unknown compound with a high RRR value, subsequently identified, was detected in derivatised form at 25.9 min with m/z 569. A number of characteristic fragment ions were also detected (m/z 275, 365, 247, 219). This metabolite was found in all six latex samples (Table 1). Due to its high RRR value in each sample, it can be expected that this metabolite contributes significantly to the properties of the latex and, presumably, to the binding of nickel in the latex. Its identification is outlined in the subsequent paragraphs.

2.4. Survey of Ni^{II} complexes in S. acuminata latex using LC–MS

Previous chromatographic analyses of the *S. acuminata* latex examined fractionated eluant from a size exclusion column (Sagner et al., 1998; Schaumlöffel et al., 2003). In the present work, the eluant was transferred directly to the electrospray source of an LC–MS instrument. This allowed a detailed study of the eluting complexes by isotope-dependant or dynamic exclusion scanning functions. The majority of the bound Ni^{II} in each latex sample eluted as citrate complexes which were detected as a broad (overloaded) peak at 35–39 min. These results are consistent with previous chromatographic separations of the latex in which most of the nickel was found associated with citrate (Lee et al., 1977; Sagner et al., 1998; Schaumlöffel et al., 2003).

The list of metabolites identified by GC–MS permitted targeted searching of the LC–MS data for Ni^{II} complexes. The molecular masses of the compounds with the highest RRR values in Table 1 allowed identification of the following gas phase complex cations (see, e.g., Fig. 2) in LC–MS chromatograms derived from the latex samples: Ni^{II}-malic acid $[Ni^{II}(C_4H_6O_5)_2(C_4H_5O_5)]^+$, Ni^{II}-itaconic acid $[Ni^{II}(C_5H_5O_4)(CH_3CN)_2]^+$, Ni^{II}-erythronic acid $[Ni^{II}(C_4H_8O_5)_2(C_4H_7O_5)]^+$, Ni^{II}-galacturonic acid $[Ni^{II}(C_6H_{10}O_7)_2(C_6H_9O_7)]^+$, Ni^{II}-tartaric acid $[Ni^{II}(C_4H_5O_6)]^+$, Ni^{II}-aconitic acid $[Ni^{II}(C_6H_6O_6)_2(C_6H_5O_6)]^+$ and Ni^{II}-saccharic acid $[Ni^{II}(C_6H_{10}O_8)(C_6H_9O_8)]^+$. The Ni^{II}-malonic acid cation $[Ni^{II}(C_3H_4O_4)_3(C_3H_3O_4)]^+$ (which is not derivatised by TMS using the method described) was also identified in the LC–MS spectra.

Table 1
Relative response ratios per gram fresh mass of each compound identified in the latex studied using GC–MS, listed in order of retention time

Metabolite	Latex sample						lg*K* (Martell and Smith, 1974)	Ni^{II} complex in LC–MS
	1	2	3	4	5	6		
Alanine	0.484	0.013	0.623	0.371	0.842	0.199		
Pyruvic acid	0.155	0.042	0.036	0.165	0.693	15.808		
2,4-Dihydroxybenzoic acid	0.002	0.001	0.001	0.006	0.002	0.053		
Glycerol	0.047	0.071	0.051	0.075	0.144	2.720		
Phosphate	0.016	0.035	0.008	0.026	0.020	0.038		
Maleic acid	**0.090**	**0.148**	**0.049**	**1.735**	**0.092**	**2.084**	**2.0**	**Yes**
Succinic acid	0.003	0.019	0.003	0.022	0.006	0.024		
Glyceric acid	0.004	0.005	0.011	0.010	0.009	0.045		
Butanedioic acid	0.004	0.005	0.011	0.010	0.009	0.045		
Itaconic acid	**0.006**	**0.008**	**0.052**	**0.125**	**0.066**	**0.001**	**1.8**	**Yes but low**
Fumaric acid	**0.027**	**0.007**	**0.119**	**0.688**	**0.026**	**0.005**	**n.a.**	**Yes**
2-Methyl-1,3-butanediol	0.00006	0.00002	0.00005	0.00002	0.00009	0.00083		
Threonic acid-1,4-lactone	0.001	0.000	0.001	0.000	0.001	0.012		
α-Ketoglutaric acid	0.004	0.006	0.001	0.003	0.002	0.082		
Erythronic acid	**0.270**	**0.384**	**0.090**	**0.187**	**0.139**	**0.089**	**n.a.**	**Yes**
2-Methyl-maleic acid	0.0022	0.0002	0.0118	0.0004	0.0386	0.0003		
Decanoic acid	0.005	0.007	0.005	0.021	0.080	0.343		
Malic acid	**0.593**	**0.416**	**0.014**	**0.384**	**0.473**	**0.370**	**3.17**	**Yes**
Threitol	0.001	0.003	0.076	0.083	0.016	0.972		
Aspartic acid	0.121	0.175	0.001	0.003	0.003	0.011		
Proline	0.648	0.785	0.000	0.049	0.033	0.007		
Butyric acid	0.012	0.057	0.001	0.013	0.013	0.004		
Succinic Anhydride	0.047	0.214	0.018	0.022	0.027	0.115		
Threonic acid	0.007	0.007	0.005	0.018	0.008	0.022		
Tartaric acid	**0.095**	**0.234**	**0.047**	**0.137**	**0.056**	**0.180**	**3.2**	**Yes**
Xylose	0.052	0.225	0.016	0.230	0.023	1.067		
Ribose	0.008	0.046	0.008	0.230	0.016	0.957		
Pentitol	0.054	0.114	0.022	0.069	0.033	0.079		
Rhamnose	0.016	0.025	0.020	0.025	0.003	0.112		
Aconitic acid	**0.180**	**0.088**	**0.533**	**0.598**	**0.692**	**0.590**	**n.a.**	**Yes**
2-Keto-L-gluconic acid	0.332	0.027	0.085	0.126	0.213	0.344		
Citric acid	**27.141**	**14.966**	**25.611**	**16.761**	**33.653**	**31.083**	**5.4**	**Yes**
Quinic acid	**2.185**	**1.161**	**4.104**	**5.241**	**4.589**	**6.398**	**n.a.**	**Same *MW* as citrate**
Fructose	0.618	4.679	0.347	1.512	0.273	9.531		
Galactose	0.075	0.004	0.040	0.033	0.060	0.631		
Glucose	0.809	0.060	0.508	0.242	0.406	0.321		
Isolated organic acid	**5.473**	**3.700**	**3.440**	**6.866**	**6.603**	**9.451**		**Yes new Ni complex**
Ascorbate	0.002	0.034	0.001	0.047	0.056	0.005		
Glucaric acid-1,4-lactone	0.377	0.203	0.210	8.424	0.309	0.759		
Galacturonic acid	**0.063**	**0.056**	**0.173**	**0.389**	**0.210**	**1.229**	**n.a.**	**Yes**
Glucopyranose	0.066	0.310	0.039	0.242	0.042	0.823		
Gluconic acid	1.745	0.024	0.023	0.024	3.834	1.429		
Saccharic acid	2.232	2.377	1.900	3.050	4.849	8.102	**4.02 (Patnaik and Panda, 1997)**	**Yes**
Fatty acid C16:0	0.067	0.093	0.062	0.168	0.510	0.454		
Myo-inositol	0.034	0.156	0.016	0.217	0.069	0.302		
3-Deoxy-arabino-Hexaric acid	0.021	0.006	0.002	0.035	0.029	0.129		
Fatty acid C18:2	0.002	0.000	0.000	0.002	0.001	0.028		
Fatty acid C18:0-OH	0.001	0.002	0.001	0.003	0.002	0.006		
Fatty acid C18:0	0.097	0.116	0.027	0.185	0.143	0.267		
Uridine	0.022	0.006	0.010	0.055	0.059	0.026		
Fatty acid C20:0	0.001	0.002	0.000	0.003	0.008	0.007		
Sucrose	**10.69**	**2.09**	**4.21**	**10.24**	**15.65**	**0.217**	**n.a.**	**with citrate**
Fatty acid C24:0	0.010	0.018	0.003	0.028	0.070	0.073		
Tetracosanol	0.001	0.001	0.001	0.002	0.006	0.005		
α-Tocopherol	0.150	0.266	0.019	1.143	0.735	1.886		
Stigmasterol	0.112	0.099	0.017	0.188	0.168	0.368		
β-Amyrin	0.076	0.060	0.046	0.600	0.189	0.529		

Bold values highlight metabolites found to be coordinated to Ni^{2+} in the LC–MS spectra.

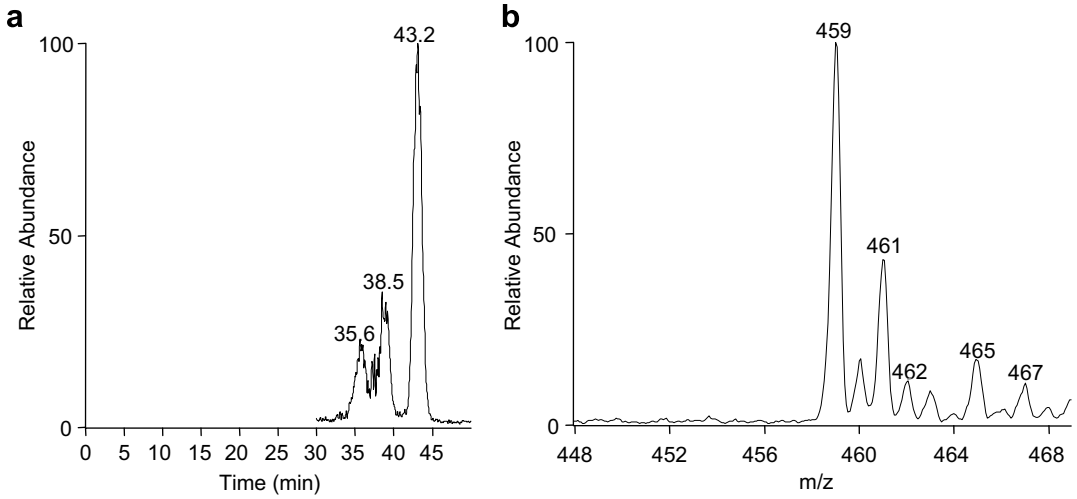

Fig. 2. (a) Base peak chromatogram *m/z* 459 of the Ni^{II} malic acid complex $[Ni^{II}(C_4H_6O_5)_2(C_4H_5O_5)]^+$ and (b) corresponding mass spectrum showing the isotope pattern of Ni^{II}.

Interestingly, the Ni^{II} nicotianamine cation $[Ni^{II}C_{12}H_{20}N_3O_6]^+$ observed previously in the latex at low levels by Schaumlöffel et al. (2003) was not detected in any of the present six samples by LC–MS.

The gas phase stoichiometry of the Ni^{II}:citrate complex was studied using CID. A number of citric acid Ni^{II} complexes were identified in both negative and positive ion mode. The dominant citrate anion with the characteristic Ni isotope pattern was observed at *m/z* 439 in the gas phase as the base peak in all latex extract eluants (Fig. 3a). Using the notation H_4cit to denote neutral citric acid, this anion could be assigned a provisional stoichiometry of $[Ni^{II} \cdot H_2cit^{2-} \cdot H_3cit^-]^-$. An anion with the same retention time and *m/z* ratio was detected in a synthetic Ni^{2+}:citrate solution of mole ratio 1:2. The MS^2 experiment for this *m/z* 439 anion resulted in Ni^{II}-bound ligand fragmentation (multiple loss of CO_2 and H_2O; Fig. 3b), consistent with the presence of two strongly bound citrate ligands. This anion is plausibly a protonated form of the $[Ni^{II}(Hcit)_2]^{4-}$ anion present in the ammonium salt characterised by X-ray diffraction (Fig. 4) (Zhou et al., 1997). A protonation equilibrium is likely to be present in the eluant solution but the specific level of protonation observed may be a function of the electrospray process. While the uncoordinated carboxylate function of $[Ni^{II}(Hcit)_2]^{4-}$ is protonated in the solid state, the carbonyl oxygen atoms of the carboxylato ligands are the likely additional protonation sites in the $[Ni^{II} \cdot H_2cit^{-2} \cdot H_3cit^-]^-$ anion detected in the gas phase.

The most pronounced Ni^{II} citrate cations, detected in the gas phase, included $[Ni^{II} \cdot H_3cit^- \cdot (CH_3CN)_2]^+$ (*m/z* 331), $[Ni^{II} \cdot H_3cit^- \cdot H_4cit]^+$ (*m/z* 441), and $[Ni^{II} \cdot H_3cit^- \cdot (H_4cit)_2]^+$ (*m/z* 633) (Fig. 3c). Cations with the same retention times and *m/z* ratios were also observed in the synthetic Ni^{II} citrate solution. The MS^2 experiment on cation $[Ni^{II} \cdot H_3cit^- \cdot (H_4cit)_2]^+$ (*m/z* 633) resulted in loss of neutral H_4cit (192 amu) with detection of $[Ni^{II} \cdot H_3cit^- \cdot H_4cit]^+$ (*m/z* 441; Fig. 3d). The MS^3 experiment on cation $[Ni^{II} \cdot H_3cit^- \cdot H_4cit]^+$ (*m/z* 441; Fig. 3e) led to ligand fragmentation. These results are again consistent with the presence in the gas phase of a protonated form $[Ni^{II} \cdot H_3cit^- \cdot H_4cit]^+$ of the anion $[Ni^{II}(Hcit)_2]^{4-}$ observed in the solid state.

A significant fraction containing Ni was detected in each latex sample at ~43.0 min, again close to the overloaded citrate peak. It corresponded to a cation of *m/z* of 591 and high resolution MS provided the molecular formula $[NiC_{18}H_{29}O_{19}]^+$. MS^2 experiments led to fragmentation consistent with loss of a sugar unit of 162 mass units, corresponding to an anhydrohexose unit. The results are consistent with the presence in the gas phase of a 1:1:1 Ni^{II}:citrate:sucrose complex cation $[Ni^{II} \cdot H_3cit^- \cdot C_{12}H_{22}O_{11}]^+$. The same experiments performed on a synthetic 1:1:1 Ni^{2+}:citric acid:sucrose solution provided equivalent results.

Another significant fraction containing Ni was detected in each latex sample (elution time ~34 min), close to the overloaded citrate peak (Fig. 5a). It corresponded to cations of *m/z* 505 and 729 (Fig. 5c), featuring the characteristic Ni isotope pattern (Fig. 5b). The MS^2 experiment on the *m/z* 729 cation yielded the *m/z* 505 ion exclusively via loss of a neutral fragment of mass 224 amu (Fig. 5d). $MS^{3,4}$ experiments on the *m/z* 505 ion resulted in fragmentation patterns (Fig. 5e and f) consistent with the decomposition of Ni^{II} bound ligands (cf, citrate complexes in Fig. 3). These observations suggest the presence in the gas phase of a 1:2 Ni:ligand complex cation with a ligand molar mass of about 224. The isolation and identification of this ligand is described below.

2.5. Isolation and characterisation of a new Ni^{2+} binding ligand

The CID experiments on the cation of *m/z* 505 discussed above suggested the presence of a 1:2 Ni:ligand complex cation with a ligand molar mass of about 224 amu. Use of a C18 column and an acidic mobile phase allowed

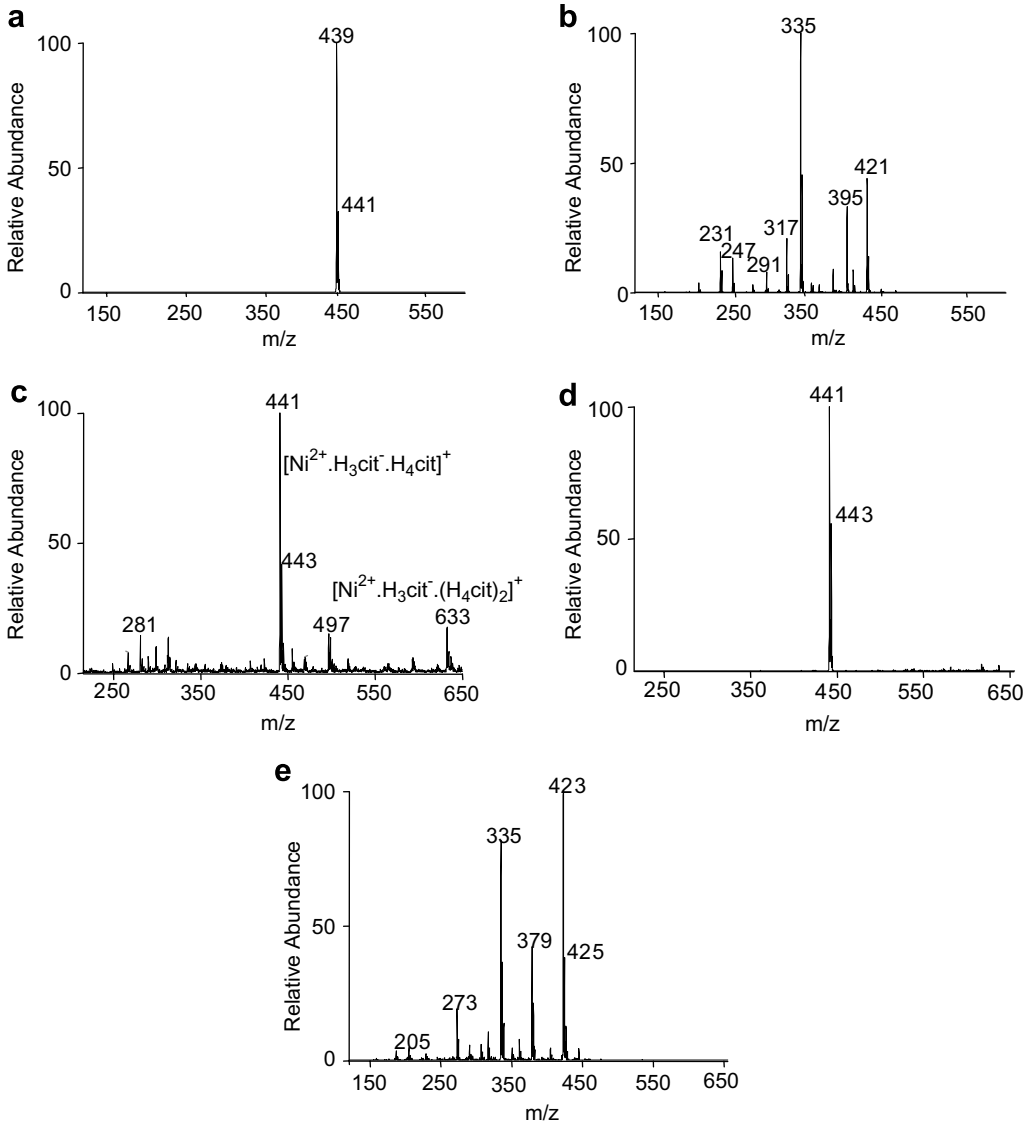

Fig. 3. CID experiments on Ni^{II}-citrate complexes isolated from latex. (a) Negative ion MS for the Ni^{II}-citrate anion $[Ni^{II} \cdot H_2cit^{2-} \cdot H_3cit^{-}]^{-}$; (b) MS^2 CID on the 439 anion; (c) full MS scan of the Ni^{II}-citrate cation $[Ni^{II} \cdot H_3cit^{-} \cdot H_4cit]^{+}$; (d) MS^2 CID of the m/z 633 cation $[Ni^{II} \cdot H_3cit^{-} \cdot (H_4cit)_2]^{+}$ and (e) MS^3 CID of the 441 cation $[Ni^{II} \cdot H_3cit^{-} \cdot H_4cit]^{+}$.

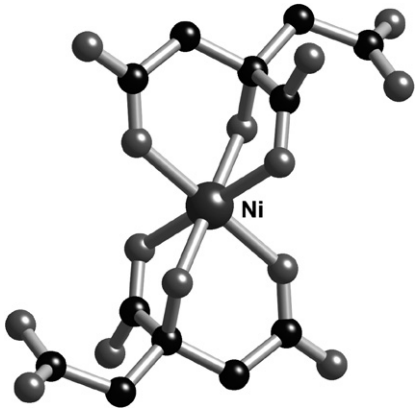

Fig. 4. The anion $[Ni^{II}(Hcit)_2]^{4-}$ detected in its ammonium salt by X-ray diffraction (Zhou et al., 1997). The uncoordinated carboxylate functions are protonated.

isolation of a fraction free of nickel. High-resolution negative ion LC Fourier transform ion cyclotron resonance (FTICR)–MS provided an anion of m/z of 223.0450, consistent with the estimate of ~224 amu (neutral ligand) from the CID experiments. A semi-preparative column was used next with an acidified mobile phase (0.1% formic acid) to increase the retention times and to improve the column resolution for protonated organic acids. Both citric acid and the putative ligand were separated for further characterisation. For the citric acid fraction, the LC-FTICR–MS technique provided a molecular mass of 191.0188 amu (theoretical for $C_6H_7O_7$, 191.0186 amu) confirming its assignment (mass accuracy, 1.05 ppm). For the putative ligand, the molecular mass in the negative ion mode was 223.0450 amu, consistent with the stoichiometry $C_7H_{12}O_8$ for the parent neutral species after losing a proton.

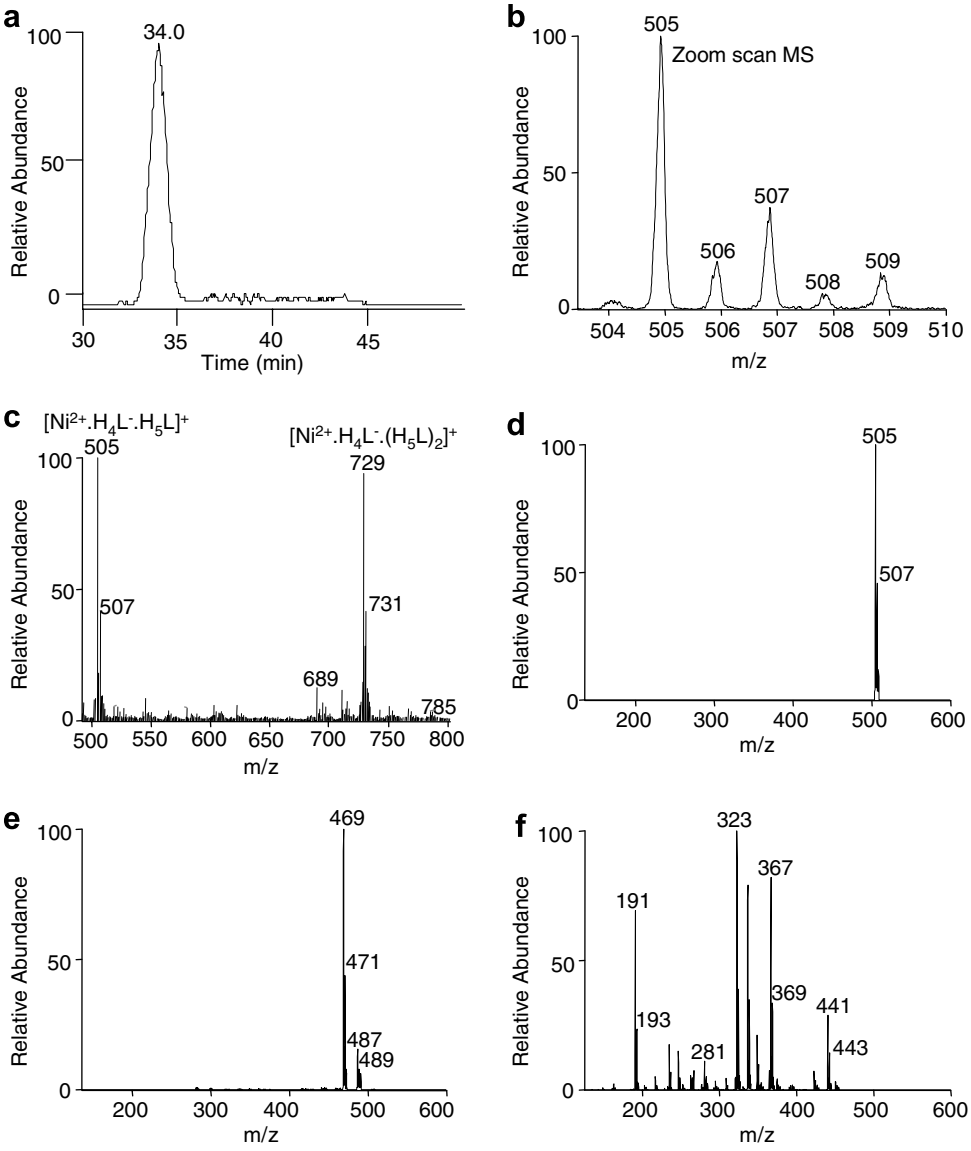

Fig. 5. (a) SEC base peak chromatogram of the Ni^{II} complex with *m/z* 505 from a latex extract of *S. acuminata*; (b) corresponding high resolution, zoom scan spectrum of the Ni^{II} complex at retention time 34.0 min; (c) full scan spectrum of the unknown Ni^{II} complex at retention time 34.0 min; (d) MS^2 CID spectrum of the *m/z* 729 cation $[Ni^{II} \cdot H_4L^- \cdot (H_5L)^2]^+$; (e) MS^3 CID spectrum of the *m/z* 505 cation $[Ni^{II} \cdot H_4L^- \cdot H_5L]^+$ and (f) MS^4 CID spectrum of the *m/z* 469 cation $[Ni^{II} \cdot H_4L^- \cdot H_5L^-H_2O]^+$.

The isolated fractions of citric acid and the unknown ligand were dissolved in 0.5 mL of D_2O and infused into the ESI source of the FTICR–MS. Deuterium exchange in the citric acid sample provided three additional peaks of +1.0063 mass units apart for each additional deuterium atom (Fig. 6a; ^{13}C is +1.0034 *m/z* units). This corresponds to three exchanged protons and, as expected, four exchangeable protons in total (including the one lost to form the observed anion). Equivalent experiments for the putative ligand were consistent with five exchangeable protons (Fig. 6b), assigned to two carboxylic acid groups and three hydroxyl groups, fitting the fragmentation pattern from the CID experiments.

Under CID conditions, the fragmentation patterns of the putative ligand and citric acid were similar apart from an extra neutral fragment for the ligand corresponding to a loss of 32 mass units. This may be assigned to CH_3OH and suggested the presence of an ether function. The total available information reduced the number of likely structures to two. NMR data (^{13}C at 200.19 MHz, D_2O and ^1H NMR at 800.13 MHz, D_2O) on the isolated fraction (<1 mg) confirmed the presence of the $C_7H_{12}O_8$ isomer 2,4,5-trihydroxy-3-methoxy-1,6-hexan-dioic acid, a methylated aldaric acid (Fig. 7a), from the following data: ^{13}C δ 58.52 (C7), 71.9 (C5), 72.0 (C2), 72.53 (C4), 82.93 (C3); ^1H δ 3.37 (H3, s, H-7), 3.51 (H1, dd, H-3), 3.94 (H1, dd, H-4), 3.96 (H1, d, H-5), 4.20 (H1, d, H-2); HSQC coupling: 72.0, 4.2 (C-2, H-2), 82.93, 3.51, (C-3, H-3), 72.53, 3.94 (C-4,H-4), 71.90, 3.96 (C-5, H-5), 58.52, 3.37 (C-7, H-7); Cosy: 4.27, 3.57 (H-2, H-3), 3.57, 4.27 (H-3, H-2) 3.57, 3.98 (H-3,

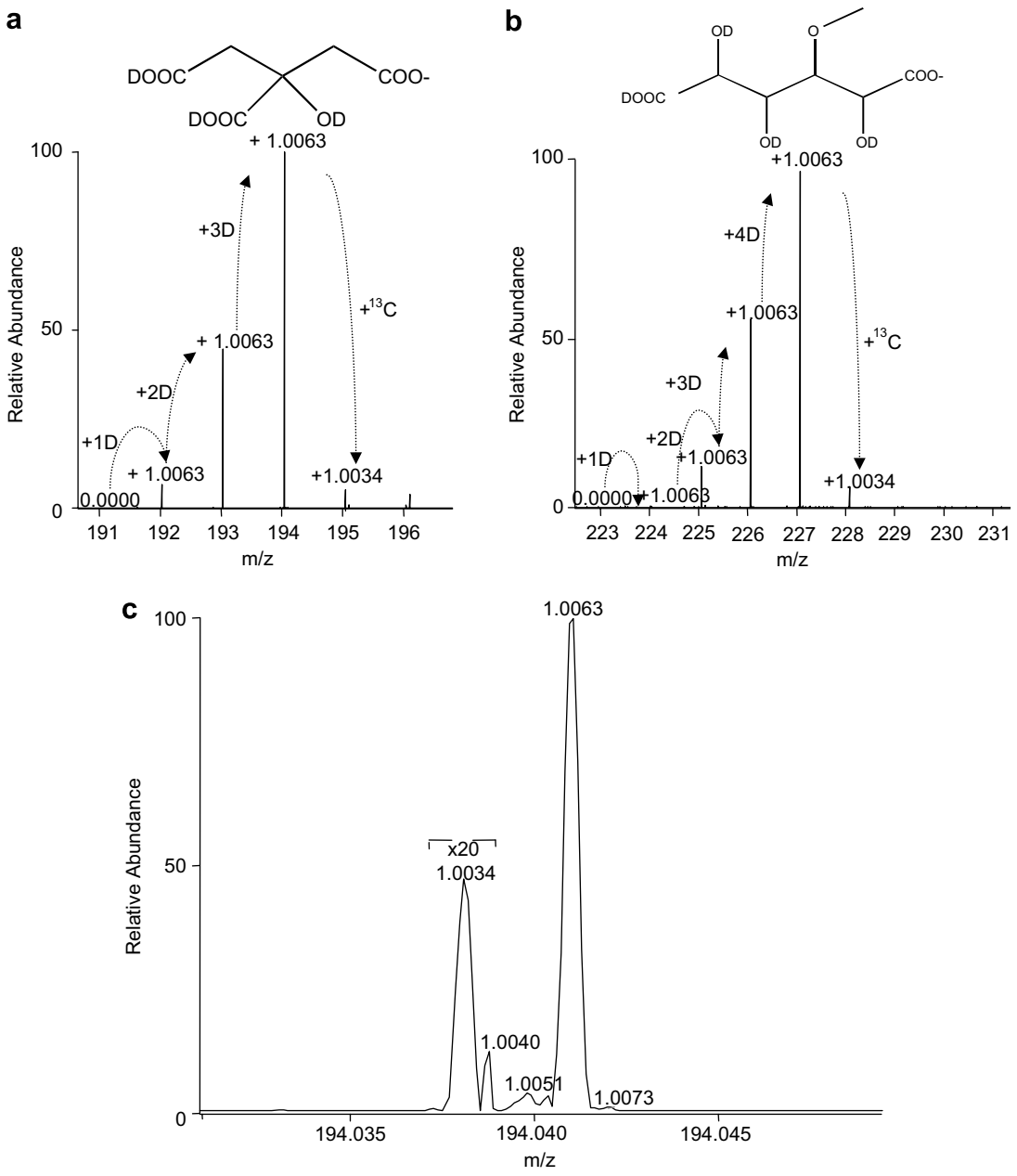

Fig. 6. Negative ion FTICR mass spectra showing the resolved peaks for the additional deuterium atoms and ^{13}C; (a) spectrum of citric acid which was isolated from latex and dissolved in D_2O; (b) spectrum of unknown ligand isolated from latex and (c) zoomed in spectra of the *m*/*z* 194 peak for citrate showing the resolution of ^{13}C and D.

H-4), 3.98, 3.57 (H-4, H-3), 3.98, 4.00 (H-4, H-5), 4.00, 3.98 (H-5, H-4), 3.41 (H7); HMBC coupling (weak signals): 3.54, 72 (H-3, C-5), 3.54, 58.6(H-3, C-7), 4.2, 82.7 (H-2, C-3), 4.2, 72.3 (H-2, C-4). It was not possible to detect the carboxylic carbon atoms due to insufficient signal. This acid has been synthesised previously (Lowendahl et al., 1975) but has never been found before in biological materials.

During the TMS derivatisation step in the GC–MS analysis, this ligand is expected to form the $[C_7H_{12}O_8 \cdot 5TMS–CH_3]^+$ ion with *m*/*z* 569. This corresponds to the metabolite with one of the highest RRR values, discussed earlier (Table 1). The GC–MS analysis of the isolated ligand using the metabolic profiling protocol produced fragmented ions corresponding to the metabolite mentioned above.

Using the notation H_5L to denote the neutral methylated aldaric acid (Fig. 7a), the cation of *m*/*z* 505 (Fig. 5) detected in the gas phase may be assigned the stoichiometry $[Ni^{II} \cdot H_4L^- \cdot H_5L]^+$ (505.0334 amu vs the experimental estimate of 505.0319 amu). By analogy with the citrate system, it is plausibly derived from an anion such as $[Ni^{II} \cdot (H_2L)_2]^{4-}$ (or a protonated form) present in aqueous solution. The tridentate ligand H_2L^{3-} plausibly binds via deprotonated C5 carboxylic acid and C4 and C5 alcohol functions (Fig. 7b).

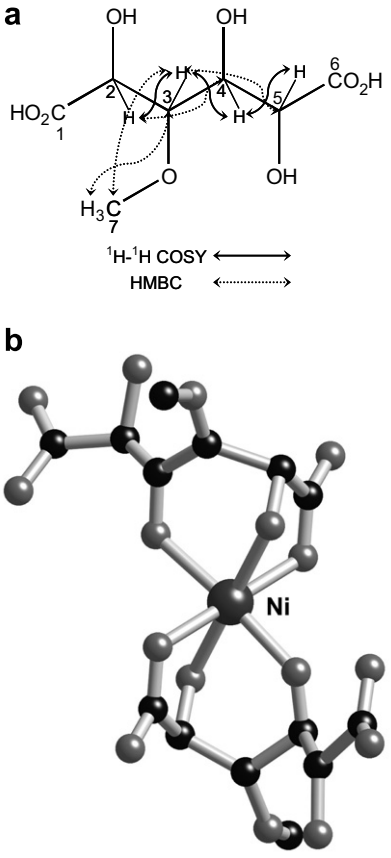

Fig. 7. (a) Proposed structure of the isolated ligand ($C_7H_{12}O_8$) showing the H–H COSY, HMBC coupling (HSQC couplings left out for clarity); 2,4,5-trihydroxy-3-methoxy-1,6-hexan-dioic acid and (b) proposed structure of the newly identified Ni^{II}-complex $[Ni^{II}C_{14}H_{23}O_{16}]^+$.

3. Conclusions

A combination of advanced MS and NMR techniques has allowed the identification of a new Ni^{II} complex in the latex of the Ni hyperaccumulator *S. acuminata*. The free ligand was isolated and structurally characterised as 2,4,5-trihydroxy-3-methoxy-1,6-hexan-dioic acid. Its high RRR suggests that this metabolite is in relatively high abundance among the other metabolites detected. MS^n experiments demonstrated that a Ni^{II} complex of stoichiometry Ni:ligand = 1:2 was present in the latex of each of the six *S. acuminata* trees sampled.

While most of the high abundance metabolites can bind to Ni^{2+}, citric acid has the highest affinity for Ni^{2+} (Table 1). The relative affinities and abundances would be expected to favour high relative concentrations of Ni^{II} citrate complexes. However, no direct correlation was apparent between the relative abundance of citric acid and the Ni concentration in the latex. There is not enough experimental evidence at present to confirm whether the other organic acids found to complex to Ni^{2+} in the extracts are actually part of the of the storage mechanism of Ni^{2+} in *S. acuminata*. However, the MS data show that a number of these acids may play an important role in this mechanism.

The present study has demonstrated the potential of using a suite of analytical approaches for non-targeted analysis on complex plant fluids. Linking data from a number of techniques (LC–MS, GC–MS, high resolution MS, NMR, ICP-OES) has allowed a more complete picture of the Ni phytochemistry in the latex of *S. acuminata* to emerge.

Future studies would involve the synthesis of the newly identified organic acid. This would enable the determination of its absolute concentration within the latex. This synthesis would be quite challenging as there are 8 stereoisomers. Also, *in vitro* binding studies could be carried out to determine its association constant with Ni^{2+}. This would help in revealing the role this ligand in Ni binding in the latex of *S. acuminata*.

4. Materials and methods

4.1. Reagents

Deionized water (18.2 MΩ cm, Millipore Synergy 185, France) and HPLC grade solvents (Sigma–Aldrich) were used for solution preparation. EDTA, citric acid, glycine, nickel nitrate, 30% hydrogen peroxide, and the NMR standard 3-(trimethylsilyl)propanoic-2,2,3,3-d_4 acid sodium salt (TSP) were all purchased from Sigma–Aldrich. The derivatisation reagents methoxyamine hydrochloride and *N*-methyl-*N*-[trimethylsilyl]trifluoroacetamide (TMS) were purchased from Biolab Ltd. (Australia). D_2O (99.9%, Cambridge Isotope Laboratory) was used in the MS and NMR studies. The LC–MS was calibrated with a mixture of caffeine, MRFA (Peptide Met–Arg–Phe–Ala) and Ultramark® 1621 (MS oligomers) (Thermo Electron Corporation) and a G2421A negative ion MS calibration solution (Agilent). The inductively coupled plasma optical emission spectrometer (ICP-OES) was calibrated with a mixed element stock standard (AM5) containing 100 mg/L of Al, As, Ba, Be, Cd, Cr, Co Cu, Fe, Pb, Mn, Ni and Zn (Choice Analytical, Australia). Deionized water solutions of 1 mg/mL ribitol and 1 mg/mL norleucine (Sigma–Aldrich) were used as internal standards in the GC–MS measurements. A pyridine (Sigma–Aldrich) solution of *n*-dodecane, *n*-pentadecane, *n*-nonadecane, *n*-docosane, *n*-octacosane, *n*-dotracontane and *n*-hexatriacontane (Sigma–Aldrich) was used to determine GC retention indices and *tris*-(perfluorobutyl)-amine (CF43, Thermo Electron Corporation) for GC–MS tuning.

4.2. Latex collection and extraction

Two of the latex samples were taken within the Parc Territorial de la Rivière Bleue and the other four samples at the same site in the southern tip of New Caledonia. Incisions were made into the bark at around shoulder height. The exuded latex was collected by pipette and stored in Eppendorf tubes (Fig. 1a and b). Samples were refrigerated

at 4 °C until analysis. Sub-samples were frozen for long term storage. Raw latex was used in the present work. For HPLC analysis, the raw latex samples (50–100 μL) were extracted with chloroform (250 μL) and deionized water (250 μL). The mixture was extracted by vortex mixing (2 min) and then centrifuged (5 min; 4500 rpm) to separate the intensely green aqueous layer from the chloroform and emulsion layers (Fig. 1c). The aqueous layer was removed and the chloroform-latex layers were re-extracted with 250 μL deionized water. The two aqueous extracts were combined for further analysis.

4.3. ICP-OES analysis

The ICP-OES measurements were conducted on a Varian Vista Pro Axial instrument with the following conditions: power 1 kW, plasma flow 15 L/min, auxiliary flow 1.5 L/min, nebuliser flow 0.9 L/min. Instrument data were evaluated using Vista Pro ICP Expert 4.1.0.

Fresh latex samples (100 mg) were weighed in conical flasks and digested with concentrated nitric acid (5 mL) by refluxing for 2 h. After cooling, 30% hydrogen peroxide (1 mL) was added to the clear solutions. Digests were then transferred to volumetric flasks and diluted to 50 mL with deionized water. A subsequent dilution (1 in 10 mL) was made with deionized water prior to analysis.

Soil samples (collected within 5 m radius from the trees to a depth of 50 cm) were dried at 60 °C for 5 days and ground to a fine powder. Triplicate samples (200 mg) were mixed with 5 mL *aqua regia* in 75 mL volumetric digestion tubes and refluxed for 3 h at 130 °C. After cooling, digests were diluted to 75 mL with deionized water and analysed for Ni by ICP-OES after a subsequent dilution (1 in 10 mL). DTPA extractions were carried out in the Soil Analysis Laboratories at IRD Noumea (New Caledonia) following the method outlined by Perrier et al. (2004). Soil samples (2.5 g) were shaken with 25 mL 1 M KCl for 1 h then centrifuged for 15 min at 2000 rpm and filtered. The residue was shaken for 1 h with a 25 mL solution of 0.005 M DTPA and 0.01 M $CaCl_2$, then centrifuged for 15 min at 2000 rpm and filtered. Both solutions were analysed for Ni by ICP-OES.

4.4. GC–MS metabolic profiling

Metabolite analysis was carried out by modifying a protocol first described by Roessner et al. (2000). Latex (10 mg) and an internal standard mixture (3 μL, ribitol and norleucine, 1 mg/ml in deionized water) were dried in vacuum. The resulting residue was derivatised in methoxyamine hydrochloride (40 μL; 30 mg/mL in pyridine; 120 min; 37 °C) followed by treatment with *N*-methyl-*N*-(trimethylsilyl)trifluoroacetamide (70 μL; 30 min; 37 °C). A standard mixture (5 μL, 0.029% (v/v) *n*-dodecane, *n*-pentadecane, *n*-nonadecane, *n*-docosane, *n*-octacosane, *n*-dotracontane and *n*-hexatriacontane dissolved in pyridine) for determining retention times was added prior to trimethylsilylation. Samples (1 μL) were injected onto the GC column using a hot needle technique. GC–MS settings used are those described earlier by Roessner et al. (2006). The GC–MS system comprised an AS 3000 autosampler, a trace GC Ultra and a DSQ quadrupole MS (Thermo Electron Cooperation, Austin, USA). The MS was tuned according to the manufacturer's recommendations using *tris*-(perfluorobutyl)-amine (CF43). GC was performed on a 30 m VF-5MS column (with 10 m Integra guard column, 0.25 μm film thickness; Varian Inc, Victoria, Australia). The chromatograms and the accompanying mass spectra were deconvoluted using an automated mass spectral deconvolution and identification system (AMDIS).

4.5. LC–MS analysis

The LC–MS system used comprised a Finnigan Surveyor LC Pump, Surveyor AutoSampler and Finnigan LCQ Deca XP Max (ThermoFinnigan, San Jose, USA). Chromatograms and mass spectra were evaluated using the Xcalibur software (ThermoElectron, Manchester, UK).

The chromatographic conditions were adapted from Schaumlöffel et al. (2003). A size exclusion column (SEC; Superdex peptide 300 × 10 mm; Pharmacia Biotech) was used for the separation of Ni^{II} complexes. Although this column is designed for the separation of molecules from 100–7000 Da, the metal complexes are charged and other mechanisms of retention such as ion exchange are expected to contribute to the overall separation process (Collins, 2004). This was seen in the SEC separation of a synthetic mixture of Ni^{II} complexes of EDTA, HBED, citric acid and glycine using the conditions described here. The components did not elute in order of decreasing molecular size. Such effects can be overcome with high ionic strength buffers. However, as the eluant is transferred directly to an electrospray MS source, high ionic strength would reduce the ionization efficiency of the analytes of interest. The mobile phase composition was optimised for separation efficiency using the synthetic mixture of Ni^{II} complexes mentioned above. The isocratic mobile phase used was a 90:10 mixture of ammonium acetate (10 mM; pH 7.0) and acetonitrile at a flow rate of 0.4 mL/min. A synthetic Ni^{II} citrate solution was infused inline with the eluant off the SEC column using a T piece connector. The MS source conditions (source position, sheath gas flow, auxiliary gas flow, capillary temperature) and ion optics (automatic tune) were then optimised with respect to the signal intensity of the Ni^{II} citrate complex. This resulted in the following optimal source conditions: sheath gas, 45 arbitrary units; auxiliary gas, 10 arbitrary units; spray voltage, 4.0 kV; capillary temperature, 300 °C. CID was carried out at 30% normalised collision energy. Mass spectra were recorded at 5 μscans/scan within a scanning range of 100–1000 m/z. A 50 μL aliquot of the latex extract was injected onto the column.

For accurate mass measurements, a linear ion trap coupled to a FTICR mass spectrometer LTQ FTMS (Finnigan

MAT, Bremen, Germany) was used. The instrument was calibrated weekly with a standard solution of caffeine, MRFA and Ultramark® 1621 in the positive ion mode and with Agilent G2421A solution for negative ion mode. For infusion of isolated fractions, a flow rate of 5 μL/min was used. ESI source conditions were optimised for different flow rates and solvents. Automatic tuning of the ion optics was conducted to maximise signal intensity for each ion of interest.

For the LC–MS measurements of free ligands, the following experimental conditions were used: C18 column (Phenomonex, Luna, 5 μm, C18, 150 × 4.6 mm), flow rate, 0.4 mL/min; gradient, 5–100% acetonitrile acidified with formic acid (0.1%) over 15 min. The following source conditions were used: sheath gas, 45 arbitrary units; auxiliary gas, 10 arbitrary units; capillary temperature, 300 °C; capillary voltage, −5 V; and tube lens voltage, −40 V. Dynamic exclusion with normalised collision energy of 35% for the CID measurements was used. In all experiments, the ion trap injection time was controlled using automatic gain control.

4.6. Semi-preparative HPLC separation

Semi-preparative HPLC separation was conducted under the following experimental conditions: C18 column (Phenomonex, Luna, C18(2), 5 μm, 250 × 10 mm), mobile phase 95:5 mixture of deionized water (0.1% formic acid) and acetonitrile (0.1% formic acid), flow rate 1 mL/min. These conditions gave good separation of citric acid from other organic acids. ESI MS was used to determine elution time for fractionation. Fractions were collected with a Gilson FC 204 (Gilson SAS, France) fraction collector. A gradient wash with acetonitrile was used to clean the column after collection of samples. The fractions were used for the isolation and characterisation of a new Ni^{2+} binding ligand.

4.7. NMR measurements

^{1}H NMR spectral data (800.13 MHz, D_2O), ^{13}C spectral data (200.19 MHz, D_2O) and the 2D spectra were recorded on an 800 MHz Bruker Biospin Avance 800 spectrometer. Chemical shifts were referenced to TSP.

Acknowledgements

We dedicate this paper to the memory of a friend, colleague and co-author Nicolas Perrier who passed away while this work was being finalised. We thank IRD Nouméa (New Caledonia) for field support and soil analysis, Ian Woodrow (School of Botany, The University of Melbourne) for loan of the semi-preparative column and Frances Separovic, David Keizer, Spencer Williams (School of Chemistry, Bio21 Molecular Science and Biotechnology Institute, The University of Melbourne) for NMR support. Damien Callahan acknowledges the Australian Research Council (ARC) (project LP0347205) and The University of Melbourne for provision of PhD and travel scholarships. We also thank the A.D. Rowden White Foundation for funding the purchase of the LC–MS instrument used in this study and the ARC Large Infrastructure Equipment and Facilities program and the Victorian Institute for Chemical Sciences for helping fund the purchase of the LTQ-FTMS.

References

AMDIS. http://chemdata.nist.gov/mass-spc/amdis/; National Institute of Standards and Technology, Gaithersburg, USA.

Baker, A.J.M., 1981. Accumulators and excluders – strategies in the response of plants to heavy metals. J. Plant Nutr. 3, 643–654.

Boyd, R.S., 1998. Hyperaccumulation as a plant defensive strategy. In: Brooks, R.R. (Ed.), Plants that Hyperaccumulate Heavy Metals. CAB International, Oxford, New York, pp. 181–201.

Boyd, R.S., Martens, S.N., 1994. Nickel hyperaccumulated by *Thlaspi montanum* var *montanum* is acutely toxic to an insect herbivore. Oikos 70, 21–25.

Callahan, D.L., Baker, A.J.M., Kolev, S.D., Wedd, A.G., 2006. Metal ion ligands in hyperaccumulating plants. J.B.I.C. 11, 2–12.

Collins, R.N., 2004. Separation of low-molecular mass organic acid-metal complexes by high-performance liquid chromatography. J. Chromatogr. A 1059, 1–12.

Davis, M.A., Pritchard, S.G., Boyd, R.S., Prior, S.A., 2001. Developmental and induced responses of nickel-based and organic defences of the nickel-hyperaccumulating shrub, *Psychotria douarrei*. New Phytol. 150, 49–58.

Dixon, N.E., Gazzola, C., Blakeley, R.L., Zerner, B., 1975. Jack bean urease (EC 3.5.1.5). Metalloenzyme. Simple biological role for nickel. J. Am. Chem. Soc. 97, 4131–4133.

Eskew, D.L., Welch, R.M., Cary, E.E., 1983. Nickel: an essential micronutrient for legumes and possibly all higher plants. Science 222, 621–623.

Hanson, B., Lindblom, S.D., Loeffler, M.L., Pilon-Smits, E.A.H., 2004. Selenium protects plants from phloem-feeding aphids due to both deterrence and toxicity. New Phytol. 162, 655–662.

Jaffré, T., Brooks, R.R., Lee, J., Reeves, R.D., 1976. *Sebertia acuminata*: a hyperaccumulator of nickel from New Caledonia. Science 193, 579–580.

Jhee, E.M., Boyd, R.S., Eubanks, M.D., 2005. Nickel hyperaccumulation as an elemental defense of *Streptanthus polygaloides* (Brassicaceae): influence of herbivore feeding mode. New Phytol. 168, 331–344.

Kopka, J., Schauer, N., Krueger, S., Birkemeyer, C., Usadel, B., Bergmueller, E., Doermann, P., Weckwerth, W., Gibon, Y., Stitt, M., Willmitzer, L., Fernie, A.R., Steinhauser, D., 2005. GMD@CSB.DB: the Golm Metabolome database. Bioinformatics 21, 1635–1638.

Lee, J., Reeves, R.D., Brooks, R.R., Jaffré, T., 1977. Isolation and identification of a citrato-complex of nickel from nickel-accumulating plants. Phytochemistry 16, 1503–1505.

Lee, J., Reeves, R.D., Brooks, R.R., Jaffré, T., 1978. The relation between nickel and citric acid in some nickel-accumulating plants. Phytochemistry 17, 1033–1035.

L'Huillier, L., Edighoffer, S., 1996. Extractability of nickel and its concentration in cultivated plants in Ni-rich ultramafic soils of New Caledonia. Plant Soil 186, 255–264.

Lowendahl, L., Petersson, G., Samuelson, O., 1975. Formation of dicarboxylic acids from 4-*O*-methyl-D-glucuronic acid in alkaline solution in the presence and absence of oxygen. Carbohydr. Res. 43, 355–359.

Martell, A.E., Smith, R.M., 1974. Critical stability constants. Plenum Press, New York.

MSRI. http://csbdb.mpimp-golm.mpg.de.
NIST. http://www.nist.gov.
Patnaik, S.M., Panda, C., 1997. Studies on complex formation of zinc-, copper-, nickel-, cobalt- and manganese(II) with D(+)-saccharic acid. J. Indian Chem. Soc. 74, 216–217.
Perrier, N., Colin, F., Jaffré, T., Ambrosi, J.P., Rose, J., Bottero, J.Y., 2004. Nickel speciation in *Sebertia acuminata*, a plant growing on a lateritic soil of New Caledonia. Comptes Rendus Geosci. 336, 567–577.
Roessner, U., Patterson, J., Forbes, M.G., Fincher, G., Langridge, P., Bacic, A., 2006. An investigation of boron toxicity in barley using metabolomics. Plant Physiol. 142, 1087–1101.
Roessner, U., Wagner, C., Kopka, J., Trethewey, R.N., Willmitzer, L., 2000. Simultaneous analysis of metabolites in potato tuber by gas chromatography–mass spectrometry. Plant J. 23, 131–142.
Sagner, S., Kneer, R., Wanner, G., Cosson, J.P., Deus-Neumann, B., Zenk, M.H., 1998. Hyperaccumulation, complexation and distribution of nickel in *Sebertia acuminata*. Phytochemistry 47, 339–347.
Schaumlöffel, D., Ouerdane, L., Bouyssiere, B., Lobinski, R., 2003. Speciation analysis of nickel in the latex of a hyperaccumulating tree *Sebertia acuminata* by HPLC and CZE with ICP MS and electrospray MS–MS detection. J. Anal. At. Spectrom. 18, 120–127.
Seregin, I.V., Kozhevnikova, A.D., 2006. Physiological role of nickel and its toxic effects on higher plants. Russ. J. Plant Physiol. 53, 257–277.
Shukla, O.P., Krishna Murti, C.R., 1971. Biochemistry of plant latex. J. Sci. Ind. Res. 30, 640–662.
Zhou, Z.-H., Lin, Y.-J., Zhang, H.-B., Lin, G.-D., Tsai, K.-R., 1997. Syntheses, structures and spectroscopic properties of nickel(II) citrato complexes, (NH4)2[Ni(Hcit)(H2O)2]2 · 2H2O and (NH4)4[Ni(Hcit)2] · 2H2O. J. Coord. Chem. 42, 131–141.